Journal of Hydrology 464–465 (2012) 79–93

Contents lists available at SciVerse ScienceDirect

Journal of Hydrology

journal homepage: www.elsevier.com/locate/jhydrol

# Integrated hydrological modeling of the North China Plain: Options for sustainable groundwater use in the alluvial plain of Mt. Taihang

Yunqiao Shu [a,c], Karen G. Villholth [b], Karsten H. Jensen [a,*], Simon Stisen [b], Yuping Lei [c]

[a] Department of Geography and Geology, University of Copenhagen, Øster Voldgade 10, 1350 Copenhagen K, Denmark
[b] Geological Survey of Denmark and Greenland, Øster Voldgade 10, 1350 Copenhagen K, Denmark
[c] Center for Agricultural Resources Research, IGDB, Chinese Academy of Sciences, 286 Huaizhong Road, Shijiazhuang 050021, China

ARTICLE INFO

*Article history:*
Received 7 April 2010
Received in revised form 21 June 2012
Accepted 25 June 2012
Available online 14 July 2012
This manuscript was handled by Geof Syme, Associate Editor

*Keywords:*
North China Plain
MIKE SHE
Groundwater
Irrigation
Evapotranspiration
Cropping pattern

SUMMARY

The integrated hydrological model MIKE SHE was applied to a part of the North China Plain to examine the dynamics of the hydrological system and to assess water management options to restore depleted groundwater resources. The model simulates the spatio-temporal distribution of recharge to and the associated dynamics of the alluvial aquifers based on climatic conditions, land use, soil characteristics, irrigation and coupled unsaturated-saturated zone processes. The model was auto-calibrated for the period 1996–2002 against daily observations of groundwater head from wells distributed across the 7230 km$^2$ region and actual evapotranspiration measured at an agricultural station located within the model area. The model simulations compared well with observations and acceptable values were obtained for both root mean square error and correlation coefficient. The calibrated model was subsequently used for scenario analysis of the effect of different cropping rotations, irrigation intensity, and other water management options, like the implementation of the South to North Water Transfer (SNWT) project. The model analysis verified that groundwater tables in the region are subject to steep declines (up to 1 m/yr) due to decades of intensive exploitation of the groundwater resources for crop irrigation, primarily the widespread crop rotation of irrigated winter wheat and mostly rainfed summer maize. The SNWT project mitigates water stress in Shijiazhuang city and areas adjacent to wastewater canals but cannot solely reverse declining water tables across the region. Combining the SNWT project and implementing region-wide crop and irrigation system changes, including deficit irrigation, wastewater irrigation, and alternating winter fallow, provides a feasible means to stabilize groundwater levels in the area.


## 1. Introduction

The North China Plain (NCP) located between 32° and 40°N, 114° and 121°E is one of the most important agricultural regions in China producing 50% of the major grains in China (World Bank, 2001). However, it is also one of the most water scarce areas in the world. The water resource per capita is approximately 500 m$^3$/yr, which is only 25% of the national average and one-fifteenth of the world average (Liu and Xia, 2004a). Due to intensification of agriculture, recurrent drought, and increased water abstraction for domestic and industrial uses, the lower reaches of many natural streams and rivers in the plains have dried up. Before the 1960s, water use in NCP was limited to that replenished by rainfall every year (average 500 mm/yr) and farmers only grew 2–3 crops every two years (Dong, 1991; Kendy et al., 2003b). With the proliferation of mechanized wells during the 1960s and onwards, groundwater became the primary water resource for industrial, domestic and agricultural use (Sun et al., 2009). Since then, the dominant cropping system switched from rainfed summer crops to mostly flood irrigated winter wheat and supplementary irrigated summer maize rotation. This rotation has been widely adopted, especially in the piedmont (foothills) of Taihang Mountains (Fig. 1). Every year, about 400 mm of groundwater is pumped for irrigation to maintain the crop production (Kendy et al., 2003a). Because this water demand exceeds the naturally renewable supply (Sun et al., 2009), water shortages have occurred widely in NCP, exacerbated by local groundwater overexploitation in urban centers. As a result, groundwater table levels have declined at a rate of nearly 1 m/yr in parts of the piedmont region of the Taihang Mountains (Kendy et al., 2003b). The average annual decline rate is reported to be 0.43 m/yr for the whole of NCP (Liu et al., 2001).

Depletion of surface water and groundwater in the NCP has severely affected the environment. Besides closure of river basins, large tracts of land that overlie cones of depression have subsided, and seawater has intruded into freshwater aquifers in coastal areas

* Corresponding author. Tel.: +45 35322484.
*E-mail address:* khj@geo.ku.dk (K.H. Jensen).

0022-1694/$ - see front matter © 2012 Elsevier B.V. All rights reserved.
http://dx.doi.org/10.1016/j.jhydrol.2012.06.048

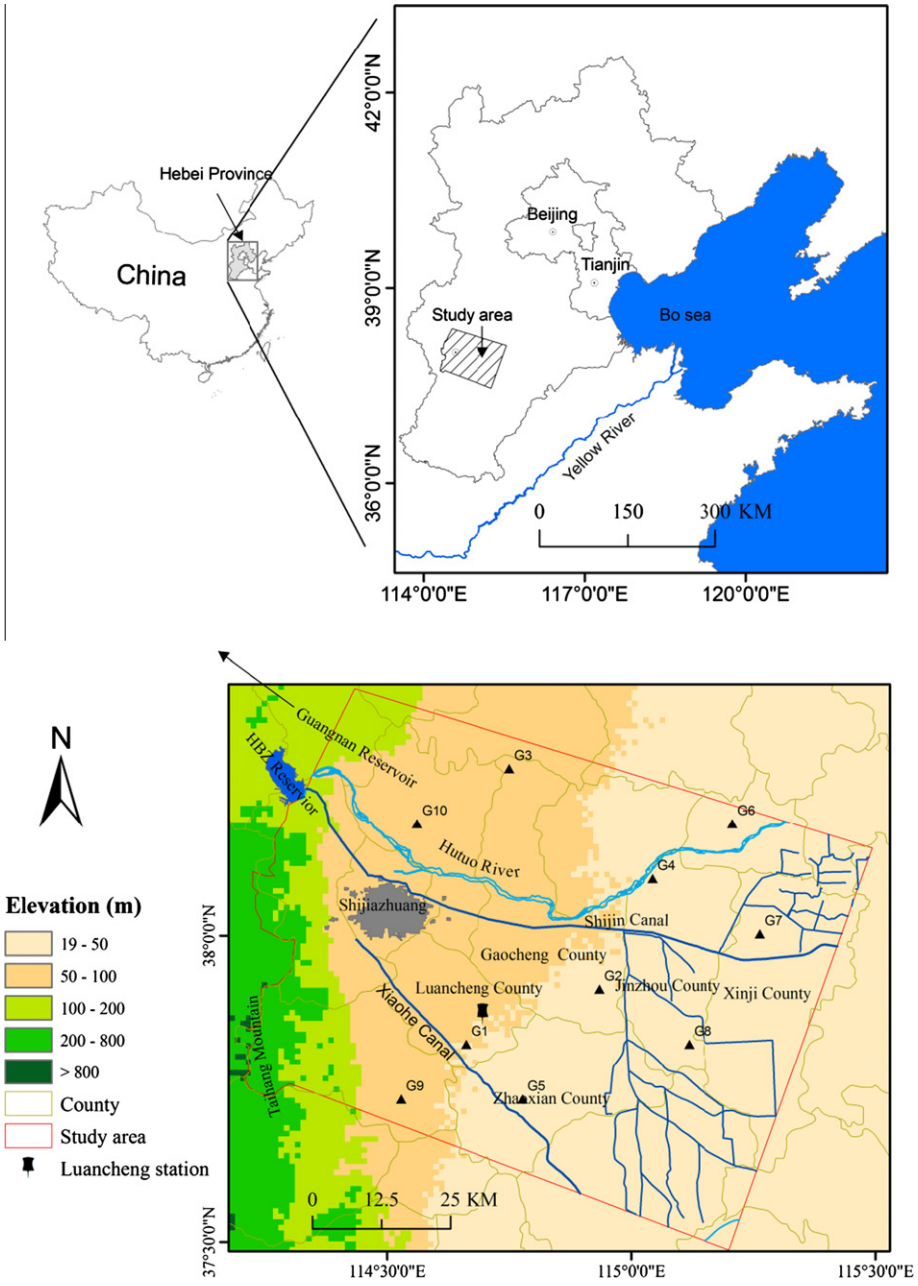


**Fig. 1.** Location of study area. Shijiazhuang City is the capital of Heibei Province. The natural Hutuo River has dried out, Shijin Canal conveys irrigation water from Huangbizhuang Reservoir, and Xiaohe Canal conveys wastewater from Shijiazhuang city. The triangles represent the groundwater observation wells.

(Liu et al., 2001). These conditions have drawn attention from researchers and organizations over the past decades (Brown and Halweil, 1998; Liu et al., 2001; Jia et al., 2002; Yang et al., 2002; Liu and Xia, 2004a,b; Kendy et al.,2007; Liu et al., 2008). Remedial measures suggested to reverse groundwater overdraft and achieve sustainable development include decreasing cropping and irrigation intensity, raising water use efficiency, increasing the use of treated wastewater, shifting water from agriculture to other, less consumptive uses, and import of transferred water.

A thorough understanding of the dynamics of the integrated soil–plant–groundwater system is key to improving the groundwater management of the NCP. The dominant components of the water balance of the groundwater system are recharge, pumping, and lateral in- and out-flows. Evapotranspiration from crop irrigation determines water losses, or consumptive losses, from the overall system in these intensively cultivated areas and indirectly controls groundwater recharge. Hence, understanding the evapotranspiration processes is critical to groundwater management in the NCP. At the same time, it is the component of the water balance that can be controlled through land use, cropping planning and irrigation application.

Controlled field experiments in lysimeters and small field plots have provided insights into the evapotranspiration processes of winter wheat and summer maize in these regions (Liu et al., 2002; Shen et al., 2002; Zhang et al., 2002). Also, one-dimensional numerical modeling of the soil water balance has provided estimates of recharge (Kendy et al., 2003b). Previous reported modeling activities of NCP, summarized in Table 1, have mainly focused on the groundwater system (Jia et al., 2002; Kendy, 2002; Mao et al., 2005; Liu et al., 2008; Wang et al., 2008) and using simple

**Table 1**
Hydrological modeling studies of North China Plain.

| Authors | Time period modeled | Area modeled | Assumption of recharge | Modeling tool | Time step | Spatial discretization |
|---|---|---|---|---|---|---|
| Jia et al., 2002 | January 1990–December 1990 | Luancheng County | Fraction of precipitation and irrigation | MODFLOW | 30 days | 30 × 30 cells 1 km × 1 km |
| Kendy, 2002 | 1949–2000 | Luancheng County | Function of precipitation plus irrigation | MODFLOW | 1-year stress periods consisting of 10 time steps | 29 × 23 cells 1 km × 1 km |
| Liu et al, 2008 | 1960–2004 | SJZ City and its surrounding seven rural counties. | Function of precipitation, infiltration, and evapotranspiration | MODFLOW | 45 years discretized into 63 stress periods | 135 × 130 cells 500 m × 500 m |
| Mao et al., 2005 | January 1990–December 1996 | Luancheng County | Fraction of precipitation, irrigation, and return flow from potholes and ponds | MODFLOW | 84 stress stages in one year | 30 × 30 cells 1 km × 1 km |
| Nakayama et al., 2006 | 1987–1988 | The Hai River catchment and the lower reach of the Yellow River | Recharge results from DSSAT-wheat and DSSAT-maize | NICE | 6 hours | 106 × 168 cells 5 km × 5 km |
| Wang et al., 2008 | 1 January 2002–31 December 2003 | The North China Plain (north to Yellow River) | Fractions of precipitation and irrigation | MODFLOW | 1 day | 147 × 162 cells 4 km × 4 km |
| This study | 1996–2002 | Alluvial plain of Mt. Taihang | Simulated by a two-layer modeling approach | MIKE SHE | Variable | 230 × 210 cells 500 m × 500 m |

approaches to estimating recharge, e.g. by assuming that recharge is a fraction of precipitation regardless of precipitation intensity or irrigation applied. Nakayama et al. (2006) developed an integrated modeling framework by coupling the biophysical and subsurface model NICE with the agricultural model DSSAT. However, the regional variation in cropping pattern and pumping for urban water supply was not considered.

Although the above model studies are able to simulate groundwater declines, they do not fully consider and integrate in a distributed manner all components of the landscape processes and human interferences that are critical for the interrelationship between precipitation, irrigation, evapotranspiration and recharge. We developed an integrated model that couples evapotranspiration, unsaturated zone and groundwater zone processes based on distributed information and data for precipitation, irrigation, potential evapotranspiration, land use, crop characteristics, soil physical data, geological settings, and pumping data. The model intrinsically accounts for the spatial and temporal distribution of recharge (from rainfall and irrigation return flows) by integrating the spatio-temporal impacts of the involved processes. The main objective of the study is to understand the groundwater dynamics as a result of present climate conditions and pumping for agricultural irrigation and urban use, and hereby to provide a sound basis for improved groundwater management. Several scenarios are evaluated with the focus on changing irrigation, cropping practices and water resources management to support a more sustainable groundwater use.

## 2. Study area characteristics

The study area is located in the piedmont of Taihang Mountains in Hebei province, which belongs to the NCP and includes the metropolitan Shijiazhuang city (population of 2.3 mill. in 2005) and its surrounding ten rural counties extending between longitude 113.82°E and 115.84°E and latitude 37.43°N and 38.48°N (Fig. 1). The 7230 km$^2$ study area is located in the center of the alluvial fan of Hutuo River and typifies the north-western NCP with intensive groundwater development for urban and rural uses. The altitude of the area varies from 800 mamsl (meter above mean sea level) in the south-western part to 20 mamsl in the eastern parts. Located in the East Asian monsoon region, it has a semi-humid and temperate climate. Average monthly temperatures range from about −4 °C in January to 25 °C in July (Liu et al., 2008). The mean annual precipitation is about 500 mm and most of the annual rainfall occurs during the humid summer months (July through September), with very little rain falling during spring and autumn, and even less during the cold, dry winters (Liu et al., 2008). The potential evapotranspiration is 1000 mm/yr or higher.

The soils of the area are considered fertile and cropping yields are relatively high for the Asian region (Villholth et al., 2009). Irrigated winter wheat and rainfed summer maize are the main two crops, together representing the most prevalent crop rotation. In addition, this area is an important producer of fruit and cotton, which are partially irrigated. The dominant natural vegetation is scrub and deciduous broad-leaved trees grow along the irrigation canals.

The main surface water resource in the region, Hutuo River, has dried out and this has exacerbated the critical problem of water scarcity. Most of the farmland is irrigated by groundwater. In addition, the eastern part of the study area is supplied with irrigation water from the distributary Shijin canal (Fig. 1) that conveys water from Huangbizhuang (HBZ) and Guangnan reservoirs (total storage capacity 1240 million m$^3$) located to the west of the study area (Fig. 1). Furthermore, some farmers use wastewater from Xiaohe canal (Fig. 1) for irrigation even though the water quality does not meet official standards.

Groundwater resources in the region are mainly found in the Quaternary sedimentary unconsolidated gravel and sand aquifers at depths down to 400 m (Fei, 1988). From west to east, the particles of the sediments become finer, and the thickness of the individual aquifers increases. Locally in the study area, the deposits are divided into four water-bearing aquifers (Zhang et al., 2003). The upper two units, extending to depths of about 50–110 m below the land surface, are unconfined, hydraulically connected and separated from the underlying aquifers by a 10–30 m confining bed. The lower two units are confined, extending to thicknesses of about 80 m in the west to 400 m towards east (Fei, 1988). Most of the wells obtain water from the two upper units (Kendy et al., 2003b).

Groundwater influx to the aquifer system is composed of lateral inflow at the foothills of Taihang Mountains and distributed vertical recharge from precipitation and irrigation return flow. Because the main natural river, Hutuo River, has dried up, it does not contribute to recharge except during extreme rainfall events. A large depression cone in hydraulic heads exists under Shijiazhuang city due to intensive groundwater pumping for urban uses.

## 3. Modeling approach

The MIKE SHE modeling system is used for the hydrological analysis of the study area. MIKE SHE, originally derived from the SHE model (Abbott et al., 1986a,b), is a deterministic, distributed physically-based hydrological model, which integrates the entire land phase of the hydrological cycle, including surface water and sub-surface water. The model simulates the spatial and temporal distribution of water resources and has been widely used for water resources and watershed planning investigations, agricultural water management, and estimation of hydrological impacts of land use changes (Jayatilaka et al., 1998; Jaber and Shukla, 2004, 2005; McMichael and Hope, 2007). The model provides the platform for development of the national water resources model for Denmark, the DK model (Henriksen et al., 2003), and it has been used for a number of groundwater investigations in Denmark (Sonnenborg et al., 2003). Due to its distributed nature, the model is well-suited for accommodating data from climate models (van Roosmalen et al., 2009) and remote sensing platforms (Andersen et al., 2002a,b; Boegh et al., 2004; Stisen et al., 2008). Given that the MIKE SHE model is complex in nature, requires comprehensive spatial and temporal data for driving it, and requires specification of many scale-dependent parameters, a number of studies have discussed issues like equifinality, parameterization, calibration and uncertainty (Beven and Binley, 1992; Feyen et al., 2000; Vazquez and Feyen, 2003; McMichael et al., 2006).

Due to the given hydrological characteristics of the study area, we applied the model in a simplified version and made certain simplifying assumptions. We are not considering river flow in the model as natural surface water is almost absent. Rather, water is assumed constantly available for local irrigation from the perennially flowing canals. Furthermore, hydraulic contact between the canals and the groundwater is assumed negligible, corresponding to the fact that most canals were lined in the early 2000s (Kendy et al., 2007), which is almost half way into the simulation period. However, we acknowledge that seepage from the canals may have had some local effects in the beginning of the simulation period. Further, we adopted the option in the model for simulating unsaturated zone processes by a two-layer water balance method (Yan and Smith, 1994), which is a relatively simple water balance method for calculating actual evapotranspiration and recharge from the unsaturated zone. The simplified evapotranspiration formulation includes the processes of interception, ponding, and evapotranspiration (van Roosmalen et al., 2009). While the unsaturated zone module of the traditional MIKE SHE model requires a detailed vertical discretization of the soil profile for solving Richards' equation, the simplified formulation assumes the unsaturated zone to consist of two layers. Details of the computational procedures are described in DHI (2007).

In addition, we assume that groundwater flow only occurs in horizontal direction and thus can be described by the two-dimensional equation for horizontal groundwater flow. Furthermore, only the upper two unconsolidated aquifer units are considered. Other studies have made the same assumption and eliminated the third dimension (Table 1) based on the reasoning that the layers of the upper unconfined aquifer are hydraulically connected, have relatively uniform hydraulic properties with depth and that most of the groundwater pumping takes place from these aquifers. Snow accumulation and melting is not considered. Although winter temperatures dip below freezing in the North China Plain, precipitation during winter is negligible.

## 4. Model input and parameterization

A regular model grid was defined for the study area with its *x*-axis oriented in NW–SE direction corresponding to the dominant groundwater flow direction (Fig. 1). The number of grid cells was $230 \times 210$ with a uniform cell size of 500 m $\times$ 500 m leading to a total model area of 12,075 km$^2$. The digital elevation model used for defining the surface topography was generated from an SRTM topographical map (http://srtm.csi.cgiar.org/), re-classified from a spatial resolution of 90 m. The confining bed separating the upper unconfined aquifer system from the underlying confined aquifers represents the lower impermeable boundary of the aquifer system. Elevation data for the lower boundary were taken from a 1:500,000 hydrogeological map of the Hebei province (HEGS, 1992).

### 4.1. Precipitation and reference evapotranspiration

Daily records from 29 precipitation gauges within the study area were available for the simulation period 1996–2002. Mean daily rainfall values for these stations are shown in Fig. 2a together with the irrigation applications. Reference evapotranspiration was estimated on a monthly basis for 15 climate stations using the FAO-56 Penman–Monteith equation (Allen et al., 1998), which has been recommended by FAO to represent potential evapotranspiration from a grass cover. The estimated monthly mean reference evapotranspiration values for the 15 climate stations are shown in Fig. 2b.

### 4.2. Soil types

The dominating soil type in the study area is loam. Sandy soil is mainly located along Hutuo River and at other isolated patches within the model area. Other sediment types like clay loam, sandy loam and loam with stones are found in few locations (Fig. 3a). The main soil physical parameters for the five main soil types are listed in Table 2. For loam and clay loam, the physical parameters determined at the Luancheng eco-agricultural station (Fig. 1) (Kendy et al., 2003b) were adopted. Parameters for the other soil types were taken from the soil catalog included in the RETC software (van Genuchten et al., 1991).

### 4.3. Land use and vegetation characteristics

Statistical data from Heibei Province (Statistical Bureau of Heibei, 1996, 1997, 1998, 2002) show that the land use of the study area has not changed notably through the time period of this study. The digital land use and land cover maps used in the model were obtained from Kang et al. (2007), who made a classification based on Moderate Resolution Imaging Spectroradiometer (MODIS) 16 day Normalized Difference Vegetation Index (NDVI) products. From the seasonal variation in NDVI, the different landscape types were identified. The study area was classified into five land use categories: winter wheat and summer maize (66%), cotton (1%), fruit tree (13%), non-vegetated land (primarily urban areas) (15%) and natural vegetation, mostly scrub (5%) (Fig. 3).

Typical ranges of values for leaf area index (LAI), crop coefficient ($K_c$) and root depth for the crop categories (winter wheat, summer maize, cotton, and fruit tree) are given in Table 3. The seasonal dynamics of the parameters for winter wheat and summer maize were determined, based on experimental data from the Luancheng station and literature values (Liu et al., 2002; Zhang et al., 2002, 2004a; Kendy et al., 2004). Winter wheat is grown from October to early June (nearly 210 days). The growth period can be divided into six stages: sowing, wintering, revival, jointing, flowering, and grain filling as shown in Fig. 4. In the same figure are also shown the growth parameters for summer maize, which is grown from June to September and has four stages: sowing, emergence, jointing-flowering, and grain-filling. The growing season for cotton is from May to October. Fruit trees include pear, apple and China

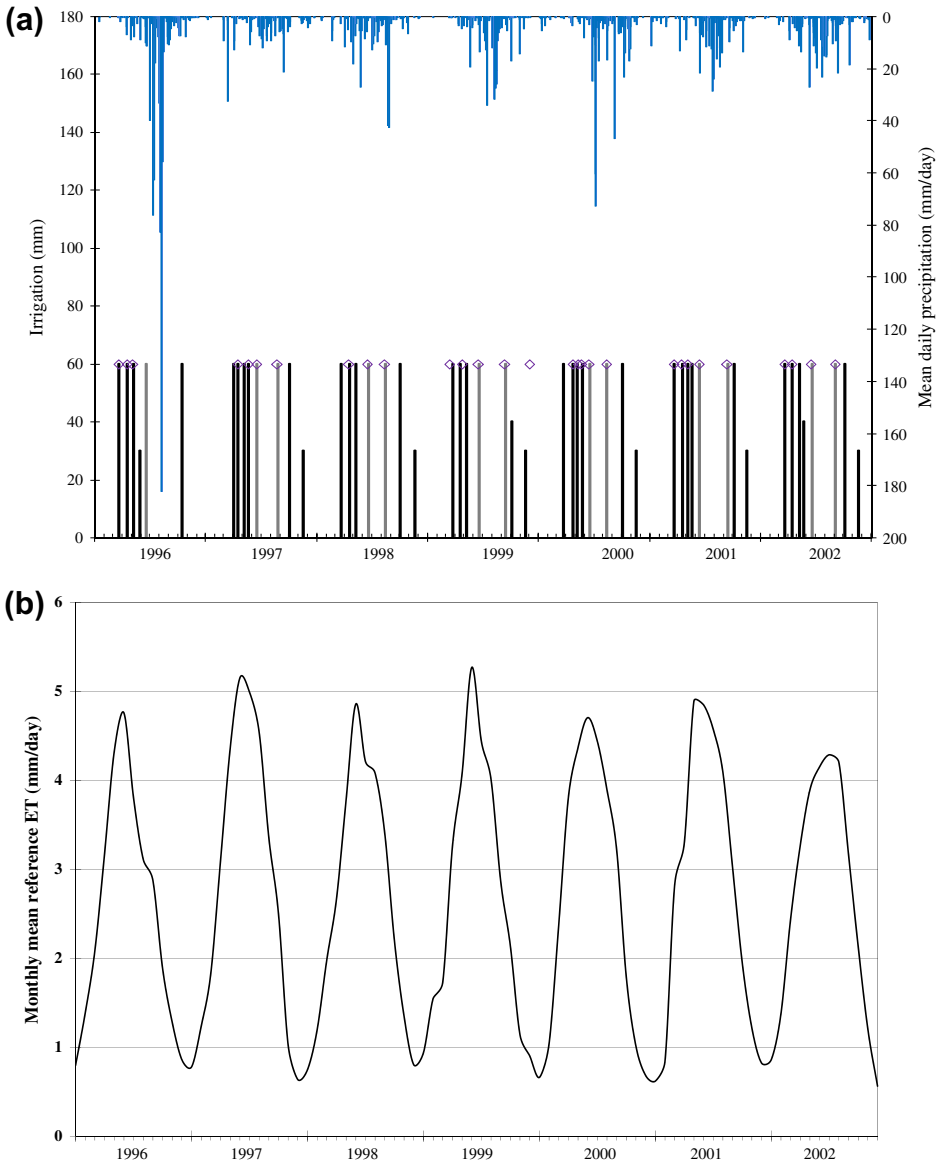


**Fig. 2.** (a) Mean daily precipitation based on observations from 29 gauging stations, applied irrigation amount for winter wheat (black line) and summer maize (gray line), and deficit irrigation (red diamonds); and (b) mean monthly reference evapotranspiration based on observations from 15 climate stations. (For interpretation of the references to color in this figure legend, the reader is referred to the web version of this article.)

date, of which most blossom in early April and ripen in the middle of September, with highest LAI and $K_c$ values in July and August.

### 4.4. Irrigation

Irrigation by groundwater was described using the shallow well option implemented in the MIKE SHE model. Using this option, water is extracted from the location (model cells) where it is used. In addition, we assumed that the Xiaohe and Shijin canals supply irrigation water to the agricultural land within 2 km proximity of the canals (Kendy et al., 2004) (Part 2 in Fig. 8) with no restriction on water accessibility and availability. Hence, these areas were not irrigated by groundwater in the model, but they received return flow from excess irrigation. Areas excepted were in the Gaocheng County where farmers reportedly stopped using canal water due to pollution (Gaocheng official website, 2005).

In the model, irrigation was applied to areas with winter wheat and summer maize, cotton and fruit trees. The exact amount of applied irrigation water and application times is unknown. However, previous studies have provided useful information on irrigation practices in the NCP (Wang et al., 2001; Liu et al., 2002; Kendy et al., 2003b; Kendy et al., 2004; Nakayama et al., 2006). Based on these studies and information of local irrigation practices collected as part of this study, generalized irrigation schemes were defined for each crop and applied for all seven years of the simulation period (1996–2002). For winter wheat and summer maize, the estimated maximum annual irrigation was 450 mm applied over a total of up to eight irrigation events. Irrigation was assumed to be applied in predefined weeks. The first seven irrigations were 60 mm and the last one 30 mm. The irrigation amounts were subject to reduction depending on the prevailing precipitation conditions within the particular weeks. If the accumulated precipitation within the preceding week was more than 30 mm, the irrigation amount was reduced by 50% and if accumulated precipitation exceeded 60 mm, no irrigation was applied. This rule led in some years to a reduction in irrigation (Fig. 2a). For winter wheat, groundwater pumping for irrigation is vital for fulfilling the water requirements due to dry winters while for the opposite

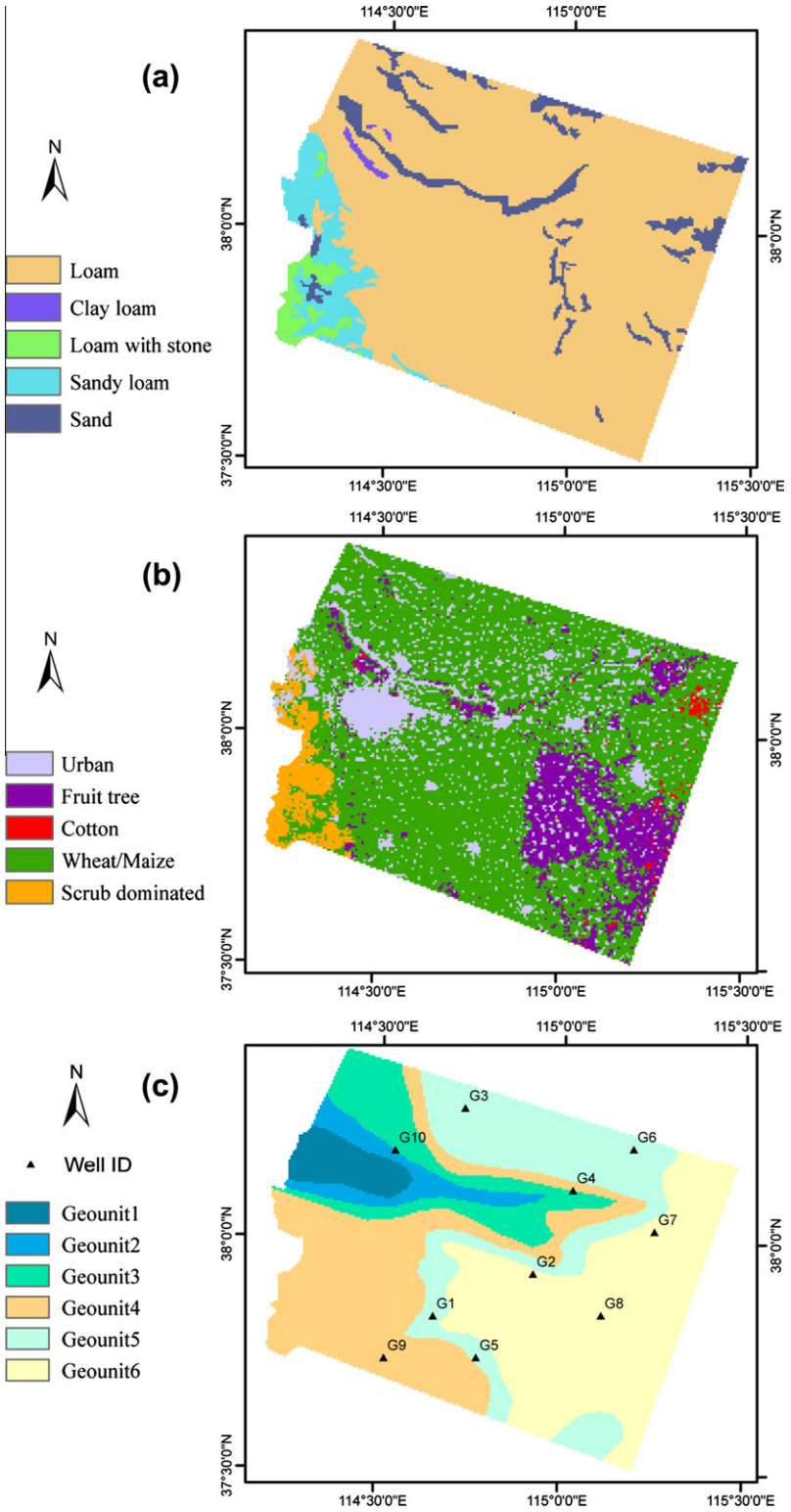


**Fig. 3.** (a) Soil types, (b) land use, and (c) geological units of the aquifer. The triangle points represent the 10 groundwater head observation wells used for calibration. The geological model shown in (c) is adopted from Liu et al. (2008).

reason summer maize is less irrigation demanding. Typical number of application events was five for winter wheat and two for summer maize. Cotton was irrigated up to twice per year for a total of 130 mm and fruit trees were irrigated up to four times for a total of 225 mm, irrespective of rainfall. In the model, irrigation was entered as additional precipitation. Irrigation intensity was low enough to not generate overland flow.

### 4.5. Groundwater zone

The hydrogeological conceptual model proposed by Liu et al. (2008) was adopted and according to this the aquifer is divided into six hydrogeological units (Fig. 3c). The grain size characteristics of these units vary from cobble-gravel to fine sand, with decreasing particle size from west to east and away from the Hutuo

**Table 2**
Soil parameterization of the two-layer model. $\theta_{sat}$, $\theta_{fc}$, and $\theta_{wp}$ are water contents at saturation, field capacity and wilting point, respectively. $K_s$ is saturated hydraulic conductivity.

| Soil type | $\theta_{sat}$ | $\theta_{fc}$ | $\theta_{wp}$ | $K_s$ (m/s) |
|---|---|---|---|---|
| Loam | 0.47 | 0.35 | 0.13 | $5.2 \times 10^{-6}$ |
| Sandy | 0.43 | 0.1 | 0.05 | $1.0 \times 10^{-4}$ |
| Sandy loam | 0.41 | 0.35 | 0.07 | $8.0 \times 10^{-6}$ |
| Clay loam | 0.42 | 0.39 | 0.14 | $3.5 \times 10^{-8}$ |
| Loam with stone | 0.45 | 0.2 | 0.08 | $8.0 \times 10^{-5}$ |

**Table 3**
Typical values for leaf area index (LAI), crop coefficient ($K_c$) and root depth for various crops.

| Crops | LAI | $K_c$ | Root depth (m) |
|---|---|---|---|
| Winter wheat | 0.5–5.0 | 0.3–1.5 | 0.8–2.0 |
| Summer maize | 1.0–4.0 | 0.3–1.4 | 0.4–1.2 |
| Cotton | 0.3–4.4 | 0–1.2 | 0.5–1.2 |
| Fruit tree | 1.0–7.0 | 0–1.0 | 3.0 |

River. All hydrogeological units have a relatively high hydraulic conductivity and are quite water-productive. Aquifer hydraulic parameter ranges are listed in Table 4, based on lithologic descriptions of aquifer materials (Jia et al., 2002; Liu et al., 2008; Wang et al., 2008b, 2009). Higher hydraulic conductivity was expected along the Hutuo River than along the edges of the alluvial fan. Due to lack of hydro-geological information near the Taihang Mountains in the south-western corner of the study area, the hydraulic characteristics in this region were estimated by extrapolation from nearby areas.

### 4.6. Groundwater pumping for industrial and domestic uses

High groundwater abstraction takes place for water supply to the Shijiazhuang metropolitan area, approximately 221 million $m^3$ in 1996 (Statistical Bureau of Heibei, 1996). Abstraction time series, based on data provided by Liu et al. (2008), were specified to the computational grid cells near the city. The abstracted water was indirectly made available again as a source of irrigation in the model through the downstream Xiaohe wastewater canal.

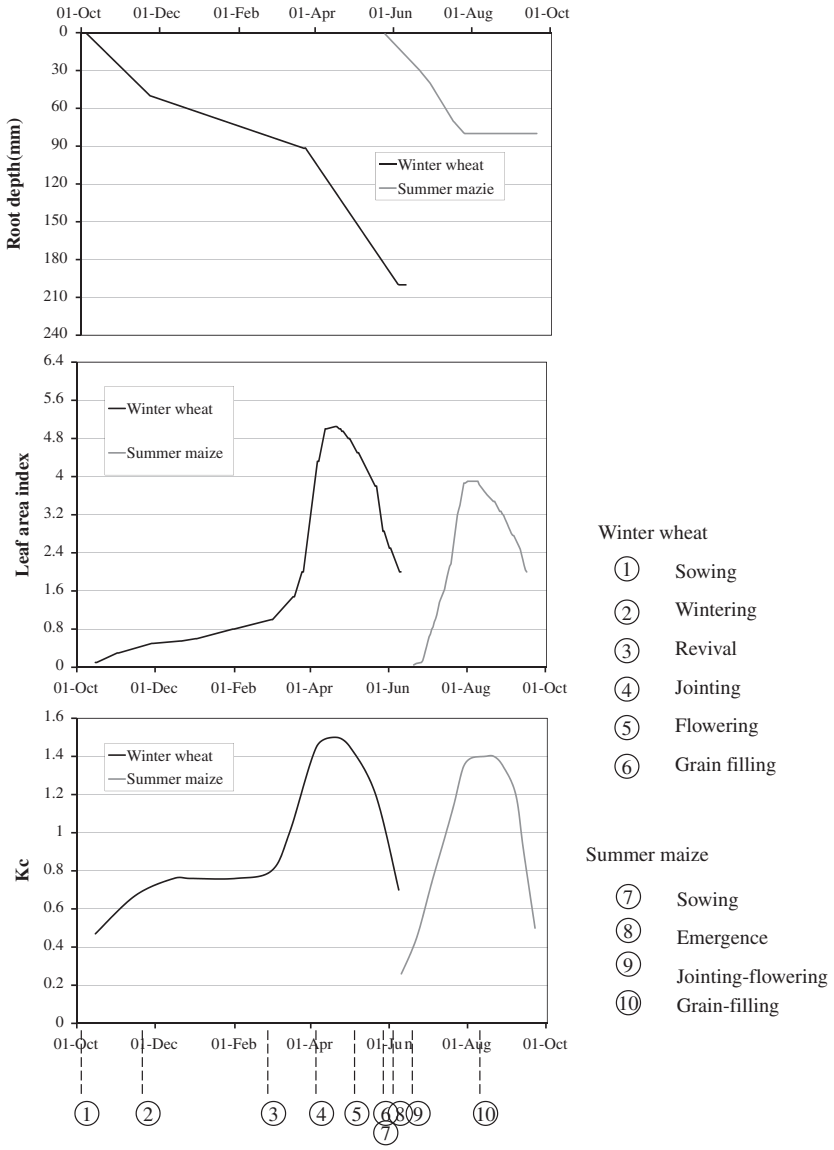


**Fig. 4.** Seasonal variation of root depth, leaf area index (LAI), and crop coefficient ($K_c$) for winter wheat and summer maize.

**Table 4**
Parameter ranges for hydraulic conductivity ($K_s$) and specific yield ($S_y$) for the individual geological units.

| Aquifer type | $K_s$ (m/s) | $S_y$ (–) | Geological units |
|---|---|---|---|
| Gravel | $3.4 \times 10^{-3}$–$4.2 \times 10^{-3}$ | 0.21–0.26 | Geounit 1 |
| Coarse sand | $1.0 \times 10^{-3}$–$3.0 \times 10^{-3}$ | 0.18–0.21 | Geounit 2 |
| Medium sand | $1.0 \times 10^{-3}$–$2.0 \times 10^{-3}$ | 0.09–0.18 | Geounit 3 |
| Sand | $9.0 \times 10^{-5}$–$1.5 \times 10^{-3}$ | 0.08–0.17 | Geounit 4, Geounit 5 |
| Fine sand | $9.0 \times 10^{-5}$–$6.0 \times 10^{-4}$ | 0.06–0.16 | Geounit 6 |

### 4.7. Initial and boundary conditions

As the hydrological model was run in dynamic mode over the seven-year simulation period (1996–2002), the initial conditions of the groundwater system were crucial for the model simulations. The aquifer system is in a transient state due to the mining of groundwater, and because the period with available observation data was short it was not possible to generate initial conditions from a preceding warm-up period as is often done in MIKE SHE applications. The initial groundwater table configuration was defined by interpolating groundwater head observations from January 1st, 1996. However, to ensure internal consistency, adjustments were made such that the initial head configuration was consistent with the specified model boundary conditions. In this process, several trial runs were made to make sure that proper initial conditions were specified and that major movement of water masses in the groundwater system did not occur at the outset of the simulations.

The model grid was oriented such that the two sides of the grid was parallel to the dominant flow direction as seen from observed interpolated hydraulic head maps (not shown). In consequence, the northwest and southeast running model boundaries (Fig. 1) were defined as no-flow boundaries. The boundary along the Taihang Mountains range was placed along the topographical divide and specified as a no-flow boundary. Inflow takes place along the most northern part of the western boundary and this was represented in the model by a specified inward decreasing hydraulic gradient (0.0025). Likewise, groundwater flowing out along the eastern boundary was represented by an outward decreasing gradient (0.0005). Both gradients were estimated from the available head observations and from previous studies (Jia et al., 2002; Liu et al., 2008; Wang et al., 2009).

### 4.8. Calibration strategy

The distributed hydrological model was calibrated using an auto-calibration tool, which is part of the MIKE SHE software package (Madsen, 2003). The calibration targets were measurements of groundwater heads, which primarily constrain the saturated zone flow, and actual evapotranspiration, which relates to soil moisture, precipitation, irrigation and groundwater recharge. Daily observations of hydraulic head from ten wells distributed across the study area (Fig. 3c) as well as daily measurements of actual evapotranspiration from a large weighing lysimeter in Luancheng station were used in the calibration procedure. The weighing lysimeter is 3 $m^2$ in area and 3 m in height. It consists of a steel box containing a soil monolith of 7.5 $m^3$ and with a total weight of about 12 t. The crop in the lysimeter was the same as grown in the surrounding land: winter wheat from October to June and summer maize from June to September. The calibration was performed on data from the period 1996 to 2002. Same weights were assigned to each of the eleven observation time series included in the calibration.

The objective function that was optimized in the auto-calibration was the root mean square error (RMSE), which is an aggregated measure that includes both the bias and the dynamic correspondence (Anderson and Woessner, 1992). The RMSE criterion is defined as:

$$\mathrm{RMSE} = \sqrt{\frac{1}{N}\sum_{i=1}^{N}(P_i - O_i)^2} \tag{1}$$

where $O$ is the observed value, $P$ is the predicted value, $i$ is the daily index, and $N$ is the total number of corresponding measurements and simulations.

The calibration results were further evaluated by five quantitative performance criteria: mean error (ME), mean absolute error (MAE), coefficient of correlation ($R$), standard deviation of residuals (STDres), and Nash–Sutcliffe model efficiency coefficient ($E$) (Nash and Sutcliffe, 1970). These criteria are defined as:

$$\mathrm{ME} = \frac{1}{N}\sum_{i=1}^{N}(O_i - P_i) \tag{2}$$

$$\mathrm{MAE} = \frac{1}{N}\sum_{i=1}^{N}|O_i - P_i| \tag{3}$$

$$R = \frac{\sum_{i=1}^{N}(O_i - \overline{O})(P_i - \overline{P})}{\sqrt{\sum_{i=1}^{n}(O_i - \overline{O})^2}\sqrt{\sum_{i=1}^{n}(P_i - \overline{P})^2}} \tag{4}$$

$$\mathrm{STD}_{\mathrm{res}} = \sqrt{\frac{1}{N}\sum_{i=1}^{N}(O_i - P_i - ME)^2} \tag{5}$$

$$E = 1 - \frac{\sum_{j=1}^{N}(O - P)^2}{\sum_{j=1}^{N}(O - \overline{O})^2} \tag{6}$$

where $\overline{O}$ is the mean observed value, and $\overline{P}$ is the mean predicted value, The five measures of model performance reflect different aspects of the degree of similarity between observations and simulations.

During the auto-calibration, model parameters were adjusted automatically according to a specific search scheme for minimizing the objective function. Details of the adopted procedure is described in Madsen (2003). The optimization algorithm is based on the shuffled complex evolution (SCE) algorithm (Duan et al., 1992), which is a global search method developed on a population-evolution search strategy. The complexity of integrated hydrological models leads to a high degree of non-linearity and consequently the objective function may be subject to several local optima. Therefore, the global search methods are assumed better

**Table 5**
Parameters selected for auto-calibration. $K_s$ (4), $K_s$ (5) and $K_s$ (6) are the hydraulic conductivities of geological units 4, 5, and 6 respectively.

| Parameter | Initial value | Lower bound | Upper bound | Final value |
|---|---|---|---|---|
| $\theta_{fc}$ For loam | 0.35 | 0.3 | 0.39 | 0.39 |
| $\theta_{wp}$ For loam | 0.13 | 0.09 | 0.20 | 0.10 |
| $K_s$ (4) | $1.0 \times 10^{-4}$ | $9.0 \times 10^{-5}$ | $1.5 \times 10^{-3}$ | $9.4 \times 10^{-5}$ |
| $K_s$ (5) | $4.0 \times 10^{-4}$ | $9.0 \times 10^{-5}$ | $1.0 \times 10^{-3}$ | $3.9 \times 10^{-4}$ |
| $K_s$ (6) | $2.0 \times 10^{-4}$ | $9.0 \times 10^{-5}$ | $6.0 \times 10^{-4}$ | $2.0 \times 10^{-4}$ |

suited for such applications than the local gradient based methods (Madsen, 2003). First, the model was subject to a manual calibration by trial-and-error. Based on the manual calibration, a formal sensitivity test was carried out using the auto-calibration tool in MIKE SHE. Twenty model parameters were examined for sensitivity and the five most sensitive parameters were chosen for further auto-calibration, comprising two parameters related to the soil-physical properties and three parameters related to the hydrogeological properties (Table 5).

## 5. Results

### 5.1. Calibration results

As shown in Table 5, the auto-calibration procedure only caused minor changes in the parameter values, suggesting that the trial-and-error calibration represented a nearly optimum set of parameter values. Table 6 lists the performance criteria computed for each of the observation stations included in the calibration. Overall, the performance criteria suggest that a reasonable calibration was obtained, albeit less favorable criteria were obtained for some observation wells. For most observations points, the correlation coefficient is above 0.9. Fig. 5 compares measured and simulated actual evapotranspiration (ET), and Fig. 6 shows measured and simulated hydraulic heads for all observation wells. The simulation results for actual ET show reasonable agreement with measurements as reflected by a correlation coefficient and model efficiency of 0.73 and 0.50, respectively (Table 6). The seasonal variation of simulated ET is in accordance with the growing seasons of winter wheat and summer maize, giving rise to two distinct annual peaks in evapotranspiration. The high values in the observational data are not reflected in the model results. The simulated daily ET is always 1–3 mm lower than measurements during high evapotranspiration periods. Previous studies have noted a similar discrepancy (Kendy et al., 2003b; Zhang et al., 2002). Due to heat conductive properties of the lysimeter's metal frame, the vegetation in the lysimeter presumably transpired more than in the surrounding field during peak periods.

Overall, the simulated groundwater dynamics show good consistency with observations (Fig. 6). All wells exhibit marked declines in groundwater heads during the seven-year period due to overexploitation of the groundwater resources. In particular, we note the excellent results for well G1 located in Luancheng County close to the eco-agricultural station. The two curves are in close agreement as also reflected by the high correlation and model efficiency values. This is encouraging, since both the soil physical parameters and the ET observations are from this site. For other wells such as G5, the observations and simulations are offset due

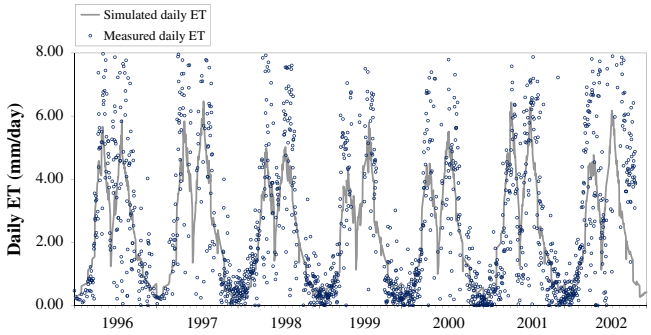


**Fig. 5.** Simulated and observed actual evapotranspiration (ET) from the lysimeter at the Luancheng agricultural experimental station.

to the modification of the initial groundwater table configuration to secure internal consistency and compliance of the imposed boundary conditions. Errors in the leveling of the wells may also be a contributing factor. The overall rate of decline agrees to a good approximation, which is considered of greater importance than the offset. Where there is a consistent lower simulated rate of decline, this could be explained by local pumping for urban uses (only considered for Shijiazhuang in the model) (e.g. G6, 8, 10). Where the simulated heads drop faster than the observations, this could be explained by recharge/seepage from the canals, which was not considered in the model (G2, 4, 5, 8). Finally, for some wells, e.g. G7, the observed short-term fluctuations in groundwater levels are not well captured by the model. The reason for this is that not all wells are standard observation wells. Some wells are most likely also pumped for irrigation and domestic use. The human impact will lead to erratic fluctuations. These local effects are not considered by the model. Moreover, the model simulations represent the mean level over a grid element of $500 \times 500$ m. In view of the above circumstances, we consider the calibration results to be acceptable for the purposes of the analysis described below.

Due to limitations in data availability, we were not able to validate the model against independent data. However, the 7-year period 1996–2002 include extreme years with both high and low precipitation. Year 1996 was an exceptionally wet year with an annual precipitation of 834 mm, year 2000 and 2002 both represent a normal year with an annual precipitation of 498 mm, while year 1997 was extremely dry with an annual precipitation of 270 mm. The high recharge in 1996 led to increases in both simulated and observed heads, and in the following year 1997 the decline in heads was higher than in other years. The general good agreement between observations and simulations for the various hydrological conditions gives confidence in the model and in part justifies the lack of independent validation.

**Table 6**
Performance results of the model calibration based on data from the period 1996 to 2002. ME: mean error, MAE: mean absolute error, RMSE: root mean squared error, STDres: standard deviation of residuals, *R*: correlation coefficient, *E*: Nash–Sutcliffe model efficiency coefficient.

| Calibration target | ME | MAE | RMSE | STDres | *R* | *E* |
|---|---|---|---|---|---|---|
| ET | 0.47 | 1.23 | 1.77 | 1.71 | 0.73 | 0.50 |
| G1 | 0.57 | 0.74 | 1.02 | 0.85 | 0.98 | 0.91 |
| G2 | −0.89 | 1.62 | 1.82 | 1.58 | 0.96 | −0.7 |
| G3 | 1.15 | 2.02 | 2.37 | 2.07 | 0.95 | −0.22 |
| G4 | 2.78 | 2.86 | 3.11 | 1.37 | 0.95 | −1.27 |
| G5 | −12.25 | 12.25 | 12.32 | 1.30 | 0.91 | −32.24 |
| G6 | 2.78 | 2.79 | 3.60 | 2.29 | 0.94 | 0.31 |
| G7 | −4.28 | 4.36 | 4.64 | 1.78 | 0.76 | −1.91 |
| G8 | −1.81 | 1.84 | 1.97 | 0.79 | 0.98 | 0.38 |
| G9 | 2.6 | 3.13 | 3.46 | 2.29 | 0.63 | −1.01 |
| G10 | −1.85 | 3.41 | 3.78 | 3.30 | 0.88 | 0.47 |

### 5.2. Water balance components

The calibrated MIKE SHE model provides important information on the water balance. In Table 7, the annual water balance components for the simulation period are listed. Groundwater pumping and precipitation are the main factors controlling the magnitude of each year's water budget. Except for the first year of the study period, which was very wet, the irrigation amount is comparable to precipitation. In combination, these two components sustain a high evapotranspiration, which is desirable from an agricultural point of view as it reflects high crop productivity. Except for years with exceptionally high precipitation, such as 1996, groundwater replenishment (recharge) is much less than pumping, which clearly undermines the long-term sustainability of groundwater use. This is also reflected in the overall constant negative water

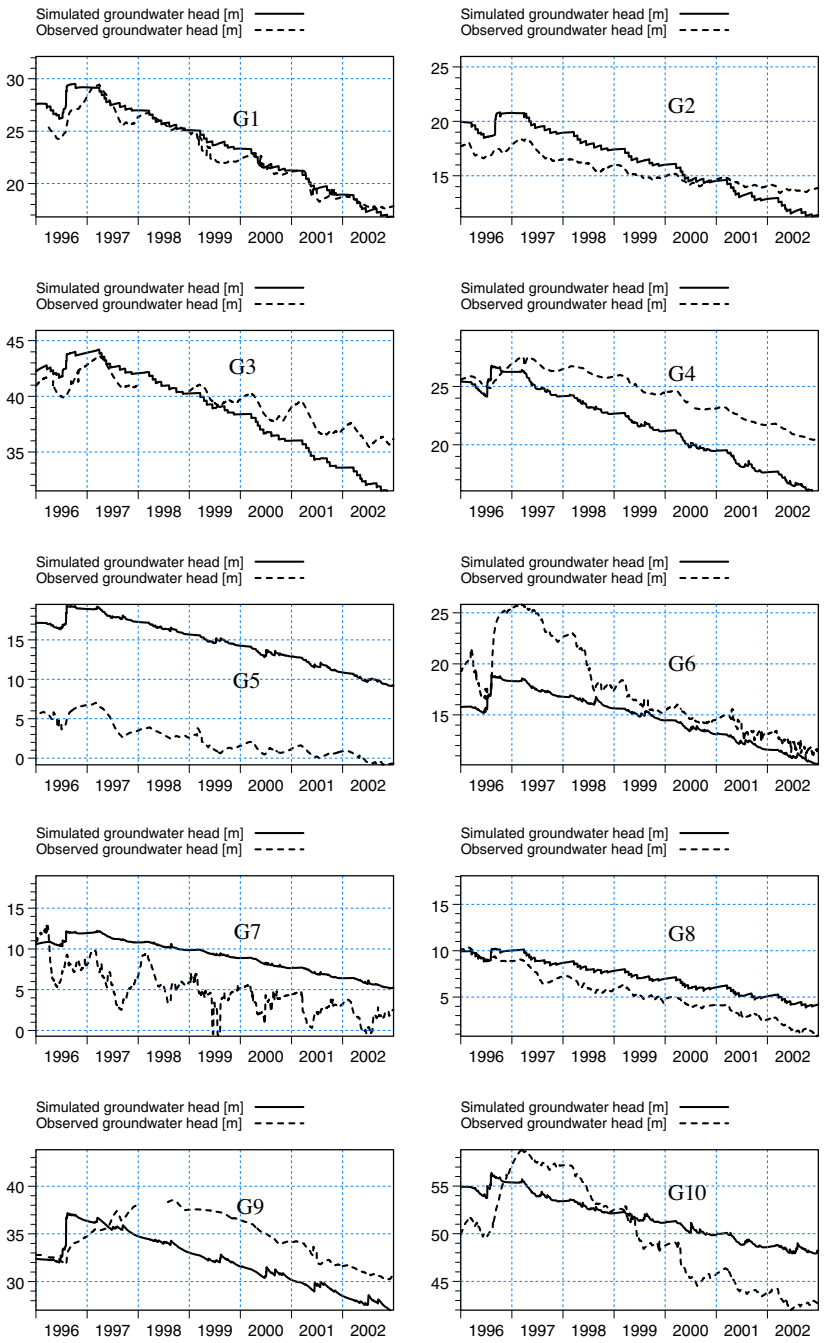


**Fig. 6.** Simulated and observed groundwater heads at 10 observation wells.

storage change in the saturated zone, except for the first year. The rate of groundwater level decline for the study period is about 1 m/yr.

Fig. 7 shows (a) observed and specified initial groundwater head distribution (January 1, 1996) as modified prior to the modeling and (b) simulated groundwater head distribution at the beginning and end of the simulation period. The depression cone under Shijiazhuang city already existed in 1996 but expanded further and deeper (simulated as a drop of more than 18 m for the seven year period) due to 180 million $m^3$ of groundwater being pumped on average annually for industrial and urban domestic uses and limited return flow. The pumping corresponds to 25 mm/yr of water over the entire study area or about 10% of the groundwater used for irrigation (on average 254 mm/yr). Hence, although local urban groundwater abstraction is of concern, the main user of groundwater and the main reason for regional groundwater level decline is irrigation. In the plain area, groundwater levels declined 4–10 m over the seven-year simulation period, most significantly in regions with winter wheat and summer maize. In the mountainous south-western part of the study area, no irrigation takes place, as the land cover is natural vegetation. The groundwater conditions in this part of the area are unknown as no observations are available. Furthermore, the terrain slopes are very steep and altogether the simulations are highly uncertain for this area. Fig. 7b shows simulated groundwater levels at the outset and after the 7-year simulation period. It is seen that the groundwater contour lines have moved upstream approximately 10 km in the lower plains, and that the cone of depression, approximately 60 m deep around

**Table 7**
Annual and mean annual simulated water balance components (mm) for the period 1996–2002.

| Year | 1996 | 1997 | 1998 | 1999 | 2000 | 2001 | 2002 | Mean |
|---|---|---|---|---|---|---|---|---|
| Precipitation | 788 | 271 | 339 | 365 | 490 | 342 | 414 | 430 |
| Actual evapotranspiration | 674 | 661 | 589 | 578 | 610 | 644 | 623 | 626 |
| Total Irrigation | 241 | 318 | 280 | 267 | 318 | 318 | 305 | 292 |
| Irrigation from canal | 32 | 40 | 37 | 35 | 41 | 41 | 40 | 38 |
| Irrigation from groundwater | 209 | 278 | 243 | 232 | 277 | 277 | 265 | 254 |
| Pumping for industry and domestic use | 30 | 27 | 26 | 24 | 24 | 21 | 21 | 25 |
| Groundwater recharge | 442 | 49 | 60 | 61 | 99 | 58 | 77 | 121 |
| Unsaturated zone storage change | −81 | −121 | −30 | −9 | 99 | −43 | 17 | −24 |
| Saturated zone storage change | 209 | −245 | −198 | −184 | −192 | −229 | −198 | −148 |
| Lateral inflow | 15 | 15 | 15 | 14 | 14 | 14 | 13 | 14 |
| Lateral outflow | 4 | 4 | 4 | 4 | 4 | 4 | 4 | 4 |

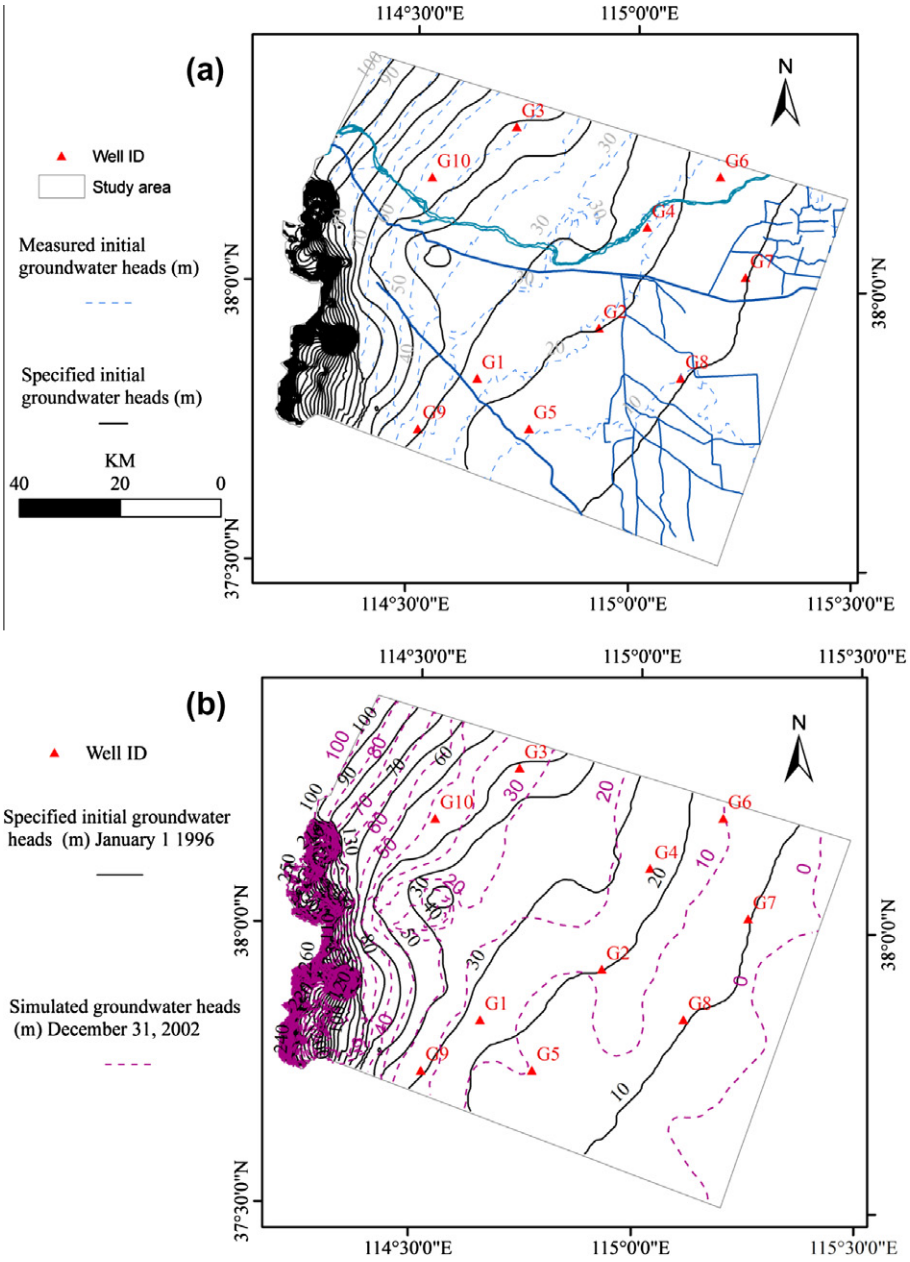


**Fig. 7.** (a) Observed and specified groundwater head configurations January 1, 1996 and (b) specified heads January 1, 1996 and simulated groundwater heads December 31, 2002.

Shijiazhuang city, has expanded further reversing flow in parts of downstream areas of the city.

### 5.3. Scenario analysis

The calibrated model was subsequently applied to investigate options and effects of various water management strategies to reduce groundwater depletion. Both supply side management (through the SNWT project) and demand side management options (through irrigation and crop management) were tested. The scenarios were driven by the climate data for 1996–2002 using the simulated groundwater levels at the end 2002 as initial conditions. Scenario results were compared with the baseline scenario, which represented the business-as-usual, i.e. a future where groundwater pumping continues unabated.

Four scenarios were drawn up. The first considered the winter wheat to be replaced by winter fallow conditions, outside the canal irrigation areas (Parts 1 and 3 in Fig. 8), everything else remaining the same. The second scenario introduced deficit irrigation to the winter wheat (Parts 1–3 in Fig. 8), whereby the number of irrigation treatments were reduced. Deficit irrigation takes advantage of the fact that crops may evapotranspire less than the potential amount, while generating unrestrained or even better crop yields if irrigated less through strategic times of their cropping cycle (Zhang et al., 2003). In our case, irrigation times (each 60 mm) were reduced from a maximum of five in the baseline scenario to a maximum of three (still subjected to reduction due to rainfall) during a dry winter wheat growing season, to two during a normal rainfall season, and one in a wet season (Fig. 2a). A wet and normal cropping season (from October to June) had a cut-off of 130 mm rainfall, and that of a normal and dry winter wheat growing season was 100 mm rainfall. Antecedent soil moisture at the time of sowing was assumed to be non-limiting and summer maize was supplementally irrigated as before. In the third scenario, the impacts of the SNWT scheme (Liu et al., 2008), which is presently under implementation, was taken into account (in addition to deficit irrigation for winter wheat as in scenario 2). The water transfer would give access to an additional 780 mill. $m^3$/yr to Shijiazhuang city (http://www.nsbd.cn/) to fully meet its present demands for municipal and industrial use (estimated to be 400 mill. $m^3$/yr (Statistical Bureau of Heibei, 2010)). The excess water was allowed to supply irrigation in additional areas along the main canals, with a total additional area of 1267 $km^2$ and 7 km further distance away from the canals (Part 3 in Fig. 8). Finally, in the fourth scenario, alternating winter fallow was introduced in Part 1 (Fig. 8), in addition to the other means in Scenarios 2 and 3. Alternating winter fallow means that winter wheat was taken out every second year in the winter wheat/summer maize growing areas away from the canal areas. In all scenarios, the cotton and fruit trees were maintained as in the base case. In combination, they contributed to 15% of the evapotranspiration over the area in the baseline scenario.

The results of the scenario simulations, in terms of average groundwater levels across the model area (except the mountain areas), are shown in Fig. 9 in conjunction with the same for the baseline scenario (scenario 0). The latter is also shown for the initial simulation and calibration period. It is seen that the blanket solution of winter fallow, basically taking winter wheat out of production except along a narrow band along the canals, significantly reduces groundwater level declines due to significant decrease in groundwater pumping and evapotranspiration. Groundwater levels stabilize with slight drops during normal years and recovery in wet years. This corroborates previous findings that winter wheat is the main culprit in groundwater depletion in NCP and that, on the other hand taking out this crop all together may not be socially and politically acceptable (Kendy et al., 2003, 2007). Hence, there is need for alternative solutions, which may attain similar, but more acceptable outcomes. From Fig. 9, it is apparent, that the proposed combination of scenarios (combined in scenario 4) may provide such viable alternative. It is also clear that avoiding the extreme measure of taking out the winter wheat requires an additional (external) source of water. Reversely, the SNTW solution will not solely substitute crop demands from groundwater.

From the cumulative water balances of the scenarios, it is seen that an annual groundwater pumping rate of 96 mm under the average of 430 mm annual precipitation over the whole region can keep the groundwater levels stable (Table 8), provided the SNWT project and other proposed measures are implemented. It is also seen that deficit irrigation (scenario 2) reduces overall irri-

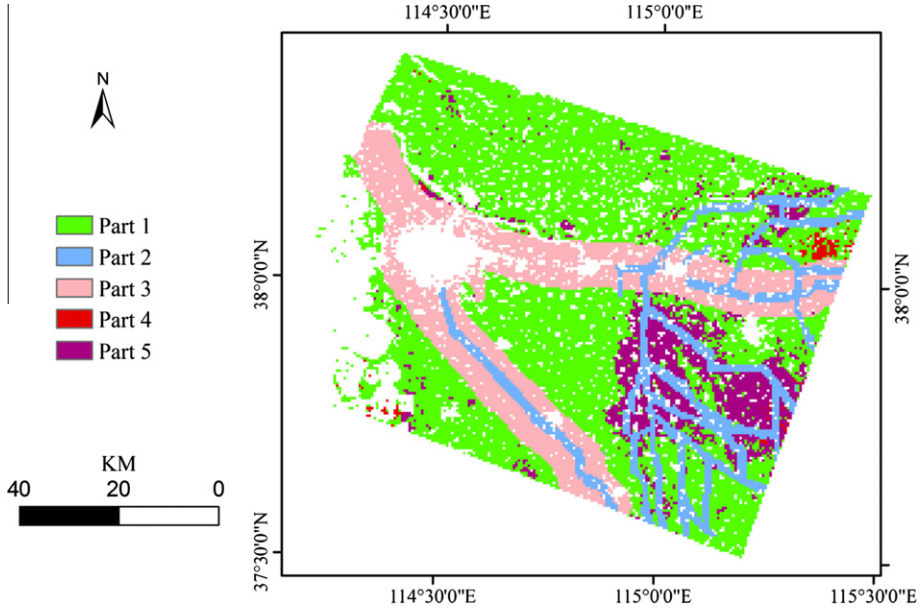


**Fig. 8.** The irrigation source for different cultivated areas. Part 1: Irrigation from shallow aquifer for winter wheat and summer maize; Part 2: Irrigation from canal via wastewater canal and reservoirs for various crops; Part 3: Irrigation from canal from SNWT project for various crops; Part 4: Irrigation from shallow aquifer for cotton; Part 5: Irrigation from shallow aquifer for fruit trees.

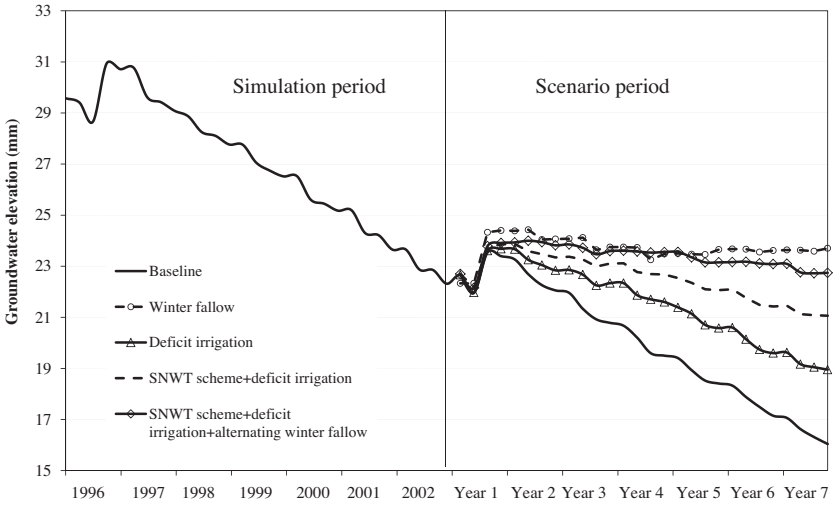


**Fig. 9.** Simulated spatially averaged groundwaer head changes for various scenarios.

**Table 8**
Mean annual water balance components (mm) during the 7-year scenario period.

| Water balance components | Scenario 0[a] | Scenario 1 | Scenario 2 | Scenario 3 | Scenario 4 |
|---|---|---|---|---|---|
| Precipitation | 430 | 430 | 430 | 430 | 430 |
| Actual evapotranspiration | 614 | 413 | 537 | 543 | 500 |
| Total Irrigation | 291 | 144 | 188 | 191 | 160 |
| Irrigation from canal | 38 | 38 | 26 | 26 | 26 |
| Irrigation from SNWT | 0 | 0 | 0 | 37 | 37 |
| Irrigation from groundwater | 253 | 107 | 162 | 127 | 96 |
| Pumping for industry and domestic use | 22 | 22 | 22 | 0 | 0 |
| Groundwater recharge | 106 | 177 | 109 | 107 | 112 |
| Unsaturated zone storage change | 0 | −14 | −28 | −29 | −23 |
| Saturated zone storage change | −160 | 57 | −65 | −15 | 22 |
| Lateral inflow | 12 | 15 | 14 | 9 | 9 |
| Lateral outflow | 4 | 4 | 4 | 4 | 4 |

[a] Scenario 0: Baseline; Scenario 1: Winter fallow; Scenario 2: Deficit irrigation; Scenario 3: SNWT scheme + deficit irrigation; Scenario 4: SNWT scheme + deficit irrigation + alternating winter fallow.

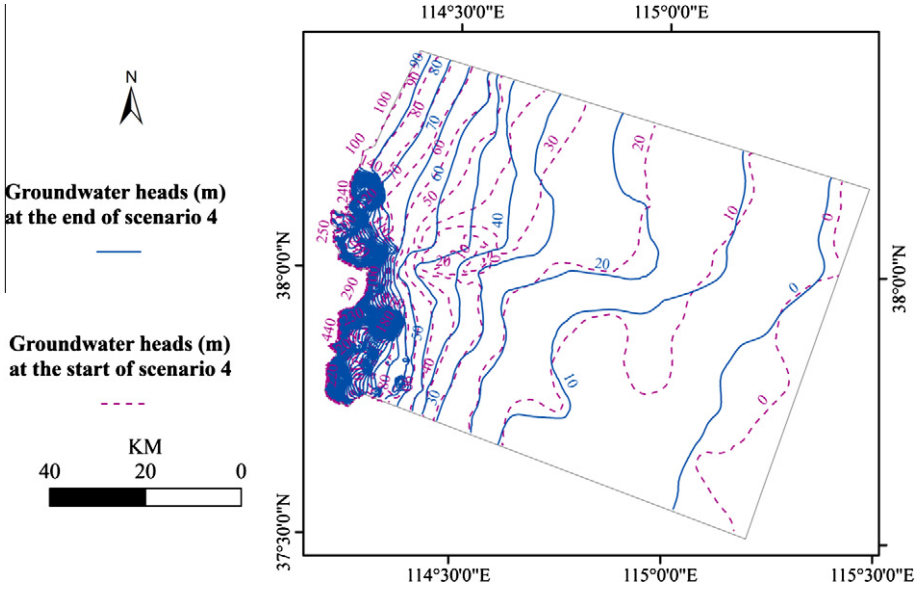


**Fig. 10.** Simulated groundwater head configurations at the start and end of scenario 4.

gation from 291 mm/yr to 188 mm/yr and evapotranspiration from 614 mm/yr to 537 mm/yr, which corresponds to a 35% saving in irrigation, but only 13% reduction in evapotranspiration. Soil moisture is also seen to decrease as a result of the introduction of deficit irrigation (unsaturated zone storage loss from 0 to 28 mm/yr). This means that replenishing soil water in the summer through rainfall becomes critical for the success of deficit irrigation (Zhang et al., 2004b; Zhang et al. 2003). From the comparison between hydraulic heads at the start and end of the scenario 4 period, a clear rebound of and practical removal of the depression cone around Shijiazhuang city is evident (Fig. 10). This is primarily a result of cessation of urban pumping. It corresponds to an approximate increase in groundwater levels near the city of about 3.4 m/yr. In the irrigated areas, the average rebound rate is negligible due to crop cultivation, but shows the stabilization of groundwater levels.

## 6. Discussion

It is clear that the options for adjusting the negative groundwater balance of the NCP involves decreasing the water depletion from beneficial and non-beneficial evapotranspiration in crop production as well as optimizing and conjunctively using existing and new sources, in urban and rural areas. The present study has evaluated measures, which in combination stabilizes the groundwater balance and the groundwater levels. Agriculture, and in particular irrigated winter wheat, is the main consumer of water, and hence measures and incentives to control this use are paramount. As the most important region in China for agricultural production and for ensuring food self-sufficiency, it is unlikely that a wide-ranging and immediate regulation and banning of winter wheat will be enforced in the NCP. However, what seems more acceptable and probable, and indeed occurring presently, is a successive societal process of adapting agriculture to increased limitations of water availability while adjusting the economy to other less water intensive livelihoods, mostly based on urbanization (Sun et al. 2009; Kendy et al., 2007). Urbanization is generally less water consumptive as well as more value-generating per water unit (Kendy et al., 2007). It is already ongoing and hence supports the transition to a less water-intense economy, but importantly it does not *per se* curtail water use in agriculture, as the economic intensification involved in urbanization still leaves land behind. This means that measures to regulate water use in agriculture are still required. As seen in the scenarios, there is scope for improving water use efficiency through better irrigation scheduling and deficit irrigation methods. Other promising measures to improve water use efficiency in winter wheat cultivation are straw mulching and deep tillage (Zhang et al., 2003). In addition, farmers are encouraged to enhance water productivity and economic returns from crop production through the switch to more high-value crops (horticulture) and use of greenhouses, especially in peri-urban areas (Foster and Garduño, 2004). Hence, urbanization goes hand in hand with agricultural intensification to optimize limited water resources. Incentives for farmers to continue farming and to maximize on land and water comes from increased food prices, increased returns from high value crops, increased energy costs for accessing groundwater, and limiting land resources. The implication of such changes is that farmers need to be entrepreneurs and well-educated to access and control water for irrigation. The mega SNWT scheme within China is helping alleviate the water supply problems in NCP. However, as shown in this paper, associated transferred amounts cannot replace current groundwater abstractions, substantiating the need for additional measures in the long term to counteract further groundwater exhaustion problems. Furthermore, the additional water resources will require better strategies and management for optimizing its use, both in the cities as well as in agriculture. Water quality becomes an overriding issue in this challenge. Likewise, new research should focus on the combined socio-economic impacts and viability of various scenarios.

## 7. Conclusions

An improved integrated dynamic and distributed hydrological modeling tool, based on the MIKE SHE code, was presented for evaluating spatio-temporal implications of water use and management options in the NCP. The primary advantage of the modeling approach is the fact that recharge and associated groundwater heads are calculated internally, based on process formulations for evapotranspiration and unsaturated-saturated flow and using measured or estimated values of precipitation, potential evapotranspiration, crop dependent irrigation, and crop, soil and hydrogeological characteristics. In addition, the model accounts for distributed land and groundwater use in both in urban and rural areas, which is critical in the NCP context.

The model was calibrated against groundwater observations and observations of evapotranspiration and it was able to provide a satisfactory simulation of the seasonal dynamics of both variables as well as the declining trend of the groundwater levels. Subsequent scenario analysis demonstrated that groundwater declines could be reversed through a suit of distributed water management measures, including deficit irrigation of winter wheat, wastewater reuse for irrigation, water transfer via the SNWT scheme, and partial alternating winter fallow. The model provides a powerful tool for sound, scientific-based groundwater management in the North China Plain.

## Acknowledgements

The work was partially supported by the International Water Management Institute (IWMI), Sri Lanka, and Knowledge Innovation Program of Chinese Academy of Sciences (KZCX2-YW-449).

## References

Abbott, M.B., Bathurst, J.C., Cunge, J.A., Oconnell, P.E., Rasmussen, J., 1986a. An introduction to the European hydrological system – Systeme Hydrologique Europeen, She .1. History and philosophy of a physically-based, distributed modeling system. Journal of Hydrology 87 (1–2), 45–59.

Abbott, M.B., Bathurst, J.C., Cunge, J.A., Oconnell, P.E., Rasmussen, J., 1986b. An introduction to the European hydrological system – Systeme Hydrologique Europeen, She .2. Structure of a physically-based, distributed modeling system. Journal of Hydrology 87 (1-2), 61–77.

Allen, R.G., Pereira, L.S., Raes, D., Smith, M., 1998. Crop evapotranspiration – Guidelines for computing crop water requirements – FAO Irrigation and drainage paper 56 <http://www.fao.org/docrep/X0490E/x0490e00.htm> FAO - Food and Agriculture Organization of the United Nations.

Andersen, J., Dybkjaer, G., Jensen, K.H., Refsgaard, J.C., Rasmussen, K., 2002a. Use of remotely sensed precipitation and leaf area index in a distributed hydrological model. Journal of Hydrology 264 (1-4), 34–50.

Andersen, J., Sandholt, I., Jensen, K.H., Refsgaard, J.C., Gupta, H., 2002b. Perspectives in using a remotely sensed dryness index in distributed hydrological models at the river-basin scale. Hydrological Processes 16 (15), 2973–2987.

Anderson, M.P., Woessner, W.W., 1992. The role of the postaudit in model validation. Advances in Water Resources 15 (3), 167–173.

Beven, K., Binley, A., 1992. The future of distributed models: model calibration and uncertainty prediction. Hydrological Processes 6 (3), 279–298.

Boegh, E., Thorsen, M., Butts, M.B., Hansen, S., Christiansen, J.S., Abrahamsen, P., Hasager, C.B., Jensen, N.O., van der Keur, P., Refsgaard, J.C., Schelde, K., Soegaard, H., Thomsen, A., 2004. Incorporating remote sensing data in physically based distributed agro-hydrological modelling. Journal of Hydrology 287 (1-4), 279–299.

Brown, L.R., Halweil, B., 1998. China's water shortage could shake world food security. World Watch, 1.

DHI, 2007. MIKE SHE User Manual Volume 2: Reference Guide, DHI Water and Environment.

Dong, K.C., 1991. The historical and social background. In: Xu, G., Peel, L.J. (Eds.), The Agriculture of China. Oxford University Press, New York, pp. 42–72.

Duan, Q.Y., Sorooshian, S., Gupta, V., 1992. Effective and efficient global optimization for conceptual rainfall-runoff models. Water Resources Research 28 (4), 1015–1031.

Fei, J., 1988. Groundwater resources in the North China Plain. Environmental Geology and Water Sciences 12 (1), 63–67.
Feyen, L., Vazquez, R., Christiaens, K., Sels, O., Feyen, J., 2000. Application of a distributed physically-based hydrological model to a medium size catchment. Hydrology and Earth System Sciences 4 (1), 47–63.
Foster, S., Garduño, H., 2004. China: towards sustainable groundwater resource use for irrigated agriculture on the North China Plain. GW-MATE CAse Profile Collection, No. 8. p. 16.
Gaocheng official website, 2005. <http://www.gc.gov.cn/>.
HEGS, 1992. Hydrogeological map of Hebei Province. Hydrogeology and Engineering Geology Survey of Hebei Province (HEGS).
Henriksen, H.J., Troldborg, L., Nyegaard, P., Sonnenborg, T.O., Refsgaard, J.C., Madsen, B., 2003. Methodology for construction, calibration and validation of a national hydrological model for Denmark. Journal of Hydrology 280 (1-4), 52–71.
Jaber, F.H., Shukla, S., 2004. Simulating water dynamics in agricultural stormwater impoundments for irrigation water supply. Transactions of the ASAE 47 (5), 1465–1476.
Jaber, F.H., Shukla, S., 2005. Hydrodynamic modeling approaches for agricultural storm water impoundments. Journal of Irrigation and Drainage Engineering-ASCE 131 (4), 307–315.
Jayatilaka, C.J., Storm, B., Mudgway, L.B., 1998. Simulation of water flow on irrigation bay scale with MIKE-SHE. Journal of Hydrology 208 (1–2), 108–130.
Jia, J.S., Yu, J.J., Liu, C.M., 2002. Groundwater regime and calculation of yield response in North China Plain: a case study of Luancheng County in Hebei Province. Journal of Geographical Sciences 12 (2), 217–225.
Kang, L.Y., Lei, Y.P., Zheng, L., Shu, Y.Q., Zhang, Q., Sun, S.W., 2007. Vegetation classification based on MODIS data and the accuracy evaluation in the pixel scale. Remote Sensing Technology and Application 22 (3), 361–366 (in Chinese).
Kendy, E., 2002. The changing ground-water balance of Luancheng County: understanding water-table declines in the North China Plain, 1949–2000: Chapter 4 in Hydrologic impacts of water-management policies on the North China Plain: case of Luancheng County, Hebei Province, 1949–2000. Cornell University, Ithaca, NY, pp. 74–108.
Kendy, E., Molden, D.J., Steenhuis, T.S., Liu, C.M., Wang, J., 2003a. Policies Drain the North China Plain: Agricultural Policy and Groundwater Depletion in Luancheng County, 1949–2000. Research Report 71. International Water Management Institute, Colombo, Sri Lanka.
Kendy, E., Gerard-Marchant, P., Walter, M.T., Zhang, Y.Q., Liu, C.M., Steenhuis, T.S., 2003b. A soil-water-balance approach to quantify groundwater recharge from irrigated cropland in the North China Plain. Hydrological Processes 17 (10), 2011–2031.
Kendy, E., Zhang, Y.Q., Liu, C.M., Wang, J.X., Steenhuis, T., 2004. Groundwater recharge from irrigated cropland in the North China Plain: case study of Luancheng County, Hebei Province, 1949–2000. Hydrological Processes 18 (12), 2289–2302.
Kendy, E., Wang, J.X., Molden, D.J., Zheng, C., Liu, C.M., Steenhuis, T.S., 2007. Can urbanization solve inter-sector water conflicts? Insight from a case study in Hebei Province, North China Plain. Water Policy 9, 75–93.
Liu, C.M., Xia, J., 2004a. Water crises and hydrology in North China – preface. Hydrological Processes 18 (12), 2195–2196.
Liu, C.M., Xia, J., 2004b. Water problems and hydrological research in the Yellow River and the Huai and Hai River basins of China. Hydrological Processes 18 (12), 2197–2210.
Liu, C.M., Yu, J.J., Kendy, E., 2001. Groundwater exploitation and its impact on the environment in the North China Plain. Water International 26 (2), 265–272.
Liu, C.M., Zhang, X.Y., Zhang, Y.Q., 2002. Determination of daily evaporation and evapotranspiration of winter wheat and maize by large-scale weighing lysimeter and micro-lysimeter. Agricultural and Forest Meteorology 111 (2), 109–120.
Liu, J., Zheng, C.M., Zheng, L., Lei, Y.P., 2008. Ground water sustainability: methodology and application to the North China Plain. Ground Water 46 (6), 897–909.
Madsen, H., 2003. Parameter estimation in distributed hydrological catchment modelling using automatic calibration with multiple objectives. Advances in Water Resources 26 (2), 205–216.
Mao, X.S., Jia, J.S., Liu, C.M., Hou, Z.M., 2005. A simulation and prediction of agricultural irrigation on groundwater in well irrigation area of the piedmont of Mt Thihang, North China. Hydrological Processes 19 (10), 2071–2084.
McMichael, C.E., Hope, A.S., 2007. Predicting streamflow response to fire-induced landcover change: implications of parameter uncertainty in the MIKE SHE model. Journal of Environmental Management 84 (3), 245–256.
McMichael, C.E., Hope, A.S., Loaiciga, H.A., 2006. Distributed hydrological modelling in California semi-arid shrublands: MIKE SHE model calibration and uncertainty estimation. Journal of Hydrology 317 (3–4), 307–324.
Nakayama, T., Yang, Y.H., Watanabe, M., Zhang, X.Y., 2006. Simulation of groundwater dynamics in the North China Plain by coupled hydrology and agricultural models. Hydrological Processes 20 (16), 3441–3466.
Nash, J.E., Sutcliffe, J.V., 1970. River flow forecasting through conceptual models part I – A discussion of principles. Journal of Hydrology 10 (3), 282–290.
Shen, Y.J., Kondoh, A., Tang, C.Y., Zhang, Y.Q., Chen, J.Y., Li, W.Q., Sakura, Y., Liu, C.M., Tanaka, T., Shimada, J., 2002. Measurement and analysis of evapotranspiration and surface conductance of a wheat canopy. Hydrological Processes 16 (11), 2173–2187.
Sonnenborg, T.O., Christensen, B.S.B., Nyegaard, P., Henriksen, H.J., Refsgaard, J.C., 2003. Transient modeling of regional groundwater flow using parameter estimates from steady-state automatic calibration. Journal of Hydrology 273 (1-4), 188–204.
Statistical Bureau of Heibei, P., 1996. Statistical Yearbook of Heibei Province 1996. Statistical Bureau of Heibei Province, Shijiazhuang.
Statistical Bureau of Heibei, P., 1997. Statistical Yearbook of Heibei Province 1997. Statistical Bureau of Heibei Province, Shijiazhuang.
Statistical Bureau of Heibei, P., 1998. Statistical Yearbook of Heibei Province 1998. Statistical Bureau of Heibei Province, Shijiazhuang.
Statistical Bureau of Heibei, P., 2002. Statistical Yearbook of Heibei Province 2002. Statistical Bureau of Heibei Province, Shijiazhuang.
Statistical Bureau of Heibei, P., 2010. Statistical Yearbook of Heibei Province 2010. Statistical Bureau of Heibei Province, Shijiazhuang.
Stisen, S., Jensen, K.H., Sandholt, I., Grimes, D.I.F., 2008. A remote sensing driven distributed hydrological model of the Senegal River basin. Journal of Hydrology 354 (1–4), 131–148.
Sun, R., Jin, M., Giordano, M., Villholth, K., 2009. Urban and rural groundwater use in Zhengzhou, China: challenges in joint management. Hydrogeology Journal 17 (6), : 1495–1506.
van Genuchten, M.T., Leij, F.J., Yates, S.R., 1991. The RETC code for quantifying the hydraulic functions of unsaturated soils.
van Roosmalen, L., Sonnenborg, T.O., Jensen, K.H., 2009. Impact of climate and land use change on the hydrology of a large-scale agricultural catchment. Water Resources Research, 45.
Vazquez, R.F., Feyen, J., 2003. Effect of potential evapotranspiration estimates on effective parameters and performance of the MIKE SHE-code applied to a medium-size catchment. Journal of Hydrology 270 (3–4), 309–327.
Villholth, K.G., Mukherji, A., Sharma, B.R., Wang, J., 2009. The role of groundwater in agriculture, livelihoods, and rural poverty alleviation in the Indo-Gangetic and Yellow River basins. In: Mukherji, A., Villholth, K.G., Sharma, B.R., Wang, J. (Eds.), Groundwater Governance in the Indo-Gangetic and Yellow River Basins: Realities and Challenges. Taylor & Francis Group, pp. 3–28.
Wang, H.X., Zhang, L., Dawes, W.R., Liu, C.M., 2001. Improving water use efficiency of irrigated crops in the North China Plain – measurements and modelling. Agricultural Water Management 48 (2), 151–167.
Wang, S.Q., Shao, J.L., Song, X.F., Zhang, Y.B., Huo, Z.B., Zhou, X.Y., 2008. Application of MODFLOW and geographic information system to groundwater flow simulation in North China Plain, China. Environmental Geology 55 (7), 1449–1462.
Wang, S., Song, X., Wang, Q., Xiao, G., Liu, C., Liu, J., 2009. Shallow groundwater dynamics in North China Plain. Journal of Geographical Sciences 19 (2), 175–188.
World Bank. 2001. Agenda for water sector strategy for North China, vol. 1, Summary report, p. 159.
Yan, J.S., Smith, K.R., 1994. Simulation of integrated surface-water and ground-water systems – model formulation. Water Resources Bulletin 30 (5), 879–890.
Yang, Y.H., Watanabe, M., Sakura, Y., Tang, C.Y., Hayashi, S., 2002. Groundwater-table and recharge changes in the Piedmont region of Taihang Mountain in Gaocheng City and its relation to agricultural water use. Water Sa 28 (2), 171–178.
Zhang, Y.Q., Liu, C.M., Shen, Y.J., Kondoh, A., Tang, C.Y., Tanaka, T., Shimada, J., 2002. Measurement of evapotranspiration in a winter wheat field. Hydrological Processes 16 (14), 2805–2817.
Zhang, X.Y., Pei, D., Hu, C.S., 2003. Conserving groundwater for irrigation in the North China Plain. Irrigation Science 21 (4), 159–166.
Zhang, X.Y., Pei, D., Chen, S.Y., 2004a. Root growth and soil water utilization of winter wheat in the North China Plain. Hydrological Processes 18 (12), 2275–2287.
Zhang, Y., Kendy, E., Yu, Q., Liu, C., Shen, Y., Sun, H., 2004b. Effect of soil water deficit on evapotranspiration, crop yield, and water use efficiency in the North China Plain. Agricultural Water Management, 64, 107–122. doi:http://dx.doi.org/10.1016/S0378-3774(03)00201-4.